Growth of GaSe ultrathin films on Si(111) substrates analyzed by the x-ray standing-wave technique

A. Koëbel, Y. Zheng, J. F. Pétroff, J. C. Boulliard, B. Capelle,* and M. Eddrief
Laboratoire de Minéralogie-Cristallographie, Universités Paris VI et Paris VII, CNRS URA009, 4, place Jussieu, 75252 Paris Cedex 5, France

(Received 8 April 1997)

The epitaxial growth of very thin GaSe films on H-Si(111), 7×7-Si(111), and $\sqrt{3}\times\sqrt{3}$ Ga-Si(111) has been investigated using the x-ray standing-wave technique. The interface structure was found to be identical whatever the Si(111) surface preparation used and consists of a GaSe half-layer. Ga atoms are covalently bonded with Si top atoms and are located in T sites. Beyond the interface, the growth proceeds layer by layer and not atomic plane by atomic plane. Moreover, the first complete layer above the interface is almost completely relaxed with respect to the Si substrate. [S0163-1829(97)07143-9]

I. INTRODUCTION

GaSe, a lamellar semiconductor studied for a long time, is currently under consideration for two purposes.

(1) A renewal of interest occurred recently[1,2] for the bulk GaSe material, because of the large infrared transparency range (from 0.65 to 18 μm) combined with high nonlinear optical coefficients [about 150 times more efficient than KDP]. Unfortunately, GaSe is a soft material with a moderate melting temperature. Nevertheless, epitaxial films on Si can still be useful for some applications.

(2) The observation of epitaxy between lamellar (2D) semiconductors,[3–5] despite strong lattice mismatches, led to hope that conventional semiconductors (referred as 3D semiconductors) could achieve epitaxy by the means of the insertion of a few 2D layers in between the 3D semiconductors.[6–10] To check this hypothesis, the nature of the interface between a 3D and a 2D semiconductor should be determined. Specifically the question is to find out if the interface is 2D or 3D-like, i.e., if it consists of weak or strong interactions. If the interface is 2D-like, the so-called van der Waals epitaxy[6,8,10,11] is obtained and the epitaxy between 3D semiconductors can be achieved via a 2D buffer. On the other hand, if the interface is 3D-like, the growth of a 3D thin film on a 2D layer with a good quality will eventually fail.

In a previous work,[12] we reported the structural analysis of GaSe thin films grown by molecular-beam epitaxy (MBE) on various Si(111) surfaces. Using high-resolution transmission electron microscopy (HRTEM), a well-defined epitaxy was found: GaSe(001)//Si(111) and GaSe[100]//Si[$1\bar{1}0$] for H-Si(111), 7×7-Si(111), and $\sqrt{3}\times\sqrt{3}$ Ga-Si(111) as well. We proposed a model of the interface where the Ga atoms are covalently bonded to Si top atoms, and a GaSe half-layer is grafted onto the Si(111) surface. Electron microscopy cannot confirm the model and another technique has to be used.

Two questions remain to be answered: (1) Is the interface structure the same for H-Si(111), 7×7-Si(111), and $\sqrt{3}\times\sqrt{3}$ Ga-Si(111) surfaces? (2) What is the growth mechanism after the interface?

To answer these questions and get a detailed description of the interface structure, two series of x-ray standing waves (XSW's) experiments were conducted. The first series dealt with H-Si(111), 7×7-Si(111), and Ga-Si(111) at submonolayer gallium coverage to determine the interface structure in each case. The second series dealt with ''thicker'' samples ranging from 1 to 3 Ga ML, one full Ga monolayer having about 7.83×10^{14} atoms per cm^2. It is generally assumed that only submonolayer adsorbates can be analyzed easily using XSW, because of the rapid drop of the measured atomic coherence due to multiple atomic sites. In this work, it will be shown that valuable information on the continuation of growth can be deduced from a XSW experiment performed on a thicker sample. This is possible, if the system is not too complicated and if a sufficient number of parameters are known in advance, especially on the submonolayer samples.

II. EXPERIMENT

A. X-ray standing waves technique

Some thirty years ago, Batterman[13,14] demonstrated the existence of XSW's inside a perfect crystal during Bragg diffraction. Further developpements[15,16] showed that the XSW's also extend above the crystal and can be used to locate the position of adsorbed atoms.

In the Bragg diffraction geometry, the XSW nodes move from the diffraction planes to between the planes as the incidence angle is scanned through the reflection curve. By monitoring the fluorescence from adsorbed atoms as the XSW moves, one can determine their positions relative to the diffraction planes.

If $R(\Delta\theta)$ is the x-ray reflectivity and $\Psi(\Delta\theta)$ the relative phase of the diffracted beam with respect to the incident beam, the normalized fluorescence yield of the atomic species α, $Y^{\alpha}(\Delta\theta)$ is written for symmetric reflection cases as

$$Y^{\alpha}(\Delta\theta)=1+R(\Delta\theta)+2\sqrt{R(\Delta\theta)}F^{\alpha}_{\vec{h}}\cos[2\pi P^{\alpha}_{\vec{h}}-\Psi(\Delta\theta)]. \quad (1)$$

Since $R(\Delta\theta)$ and $\Psi(\Delta\theta)$ are given by the dynamical theory, the only parameters are $F^{\alpha}_{\vec{h}}$ and $P^{\alpha}_{\vec{h}}$, the amplitude and phase of the Fourier coefficient of the atomic distribution of the atomic α species. They are related by

 © 1997 The American Physical Society

$$F_{\vec{h}}^{\alpha} e^{2i\pi P_{\vec{h}}^{\alpha}} = \frac{\sum_{j=1}^{N^{\alpha}} e^{2i\pi \vec{h}\cdot\vec{r}_j} e^{-M_j^{\alpha}}}{N^{\alpha}}, \tag{2}$$

where $\vec{h}$ is the diffraction vector, $\vec{r}_j$ the position of atom j with respect to the diffraction planes, N^{α} the number of atoms of the species α, and M_j^{α} the Debye-Waller factor of the jth atom of the species α. The coefficient $F_{\vec{h}}^{\alpha}$ will hereafter be referred to as coherent fraction and the coefficient $P_{\vec{h}}^{\alpha}$, expressed between 0 and 1, will be referred to as coherent position.

In the case of a perfectly ordered adsorbate on a unique atomic site, $F_{\vec{h}}^{\alpha}$ is near 1 and $P_{\vec{h}}^{\alpha}$ is a relative measure of the distance between the targeted atom and the nearest diffraction plane. For a disordered distribution, still comporting one unique atomic site $F_{\vec{h}}^{\alpha}$ drops from 1 to 0, giving the proportion of ordered atoms on the surface. If there is more than one site, these numbers cannot be interpreted as simply and the values of $F_{\vec{h}}^{\alpha}$ should be decomposed into two components, one representing the order of the atomic distribution and the other the site multiplicity. For a two positions case, $F_{\vec{h}}^{\alpha}$ is given by

$$F_{\vec{h}}^{\alpha} = 2F_0^{\alpha} |\cos(2\pi\Delta P_{\vec{h}}^{\alpha})|, \tag{3}$$

where F_0^{α} is the disorder contribution ranging from 1 to 0 and $\Delta P_{\vec{h}}^{\alpha}$ the difference between the two positions measured along direction $\vec{h}$. Even for a perfect sample with F_0^{α} near 1, a low coherent fraction can still be measured if there is more than one site. The study of those coherent fractions in multisite cases can lead to the knowledge of specific atomic positions that cannot be obtained using coherent positions only.

B. GaSe structure and sample preparation

GaSe structures can be described as a stacking of layers, each layer consisting of four two-dimensional sheets of atoms in the sequence Se-Ga-Ga-Se. The layers are bonded together by weak van der Waals interactions while intralayer bonds are of a covalent type. Different ways of stacking the layers induce various polytype structures. For bulk GaSe, β type and ϵ type with two layers per unit cell are commonly encountered (β,[17] $P6_3/mmc$, $a=3.75$ Å, $c=15.99$ Å; ϵ, $P\overline{6}m2$, $a=3.74$ Å, $c=15.89$ Å). Films grown on silicon usually exhibit the γ structure[18] ($R3m$, $a=3.74$ Å, $c=23.86$ Å, with three layers per unit cell).

If the silicon substrate is taken as reference, there are different ways to build the GaSe/Si heterostructure. First, GaSe[100] may be parallel or antiparallel to Si[$1\overline{1}0$]. This operation is a 180° rotation around the GaSe $\vec{c}$ axis. These two heterostructures have different stacking orientations and different layer configurations as well. The other two different heterostructures are obtained using a (001) mirror operation on the two previous heterostructures. This operation does not change the layer configuration but changes the stacking orientation. On the four found structures, two stacking orientations are visible. For each stacking orientation, two configurations of the layer are possible but have not been recognized with HRTEM.

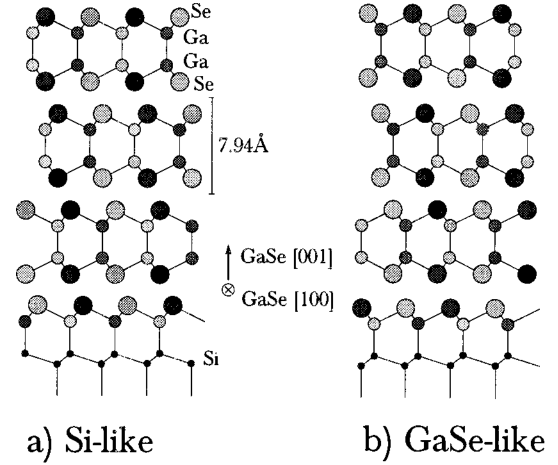

FIG. 1. Schematic of a heterostructure between the γ-GaSe polytype and Si. With the same stacking sequence, each layer, including the one near the interface, may have two different configurations, namely, Si-like (a) or GaSe-like (b). Besides that from the orientation within a layer, two different stacking sequences may appear, giving rise to four different heterostructures.

If one half-layer is present at the interface, it may present those two different configurations that are determined with the Se position (see Fig. 1). The Se may be in a site with no silicon atom in the Si layer underneath, like a Si itself in its structure [Si-like structure, Fig. 1(a)] or may be like in the GaSe structure with one atom present in the underneath Si layer [GaSe-like, Fig. 1(b)]. After this half-layer, the stacking may have two directions. HRTEM observations clearly demonstrated the existence of both stacking sequences in equal proportions but cannot conclude if both orientations possess one single-layer configuration or two.

The samples were prepared by MBE using a 2300 Riber system[10] and *in situ* reflection high-energy electron diffraction (RHEED) observations were performed. The substrates were 2-mm-thick 2-in.-diam Si(111) wafers polished on both sides. The surfaces were prepared using a modified Shiraki method that leaves a clean H-Si(111) surface. 7×7-Si(111) surfaces were obtained in heating the H-Si(111) samples up to 750 °C. $\sqrt{3}\times\sqrt{3}$ Ga-Si(111) were obtained in depositing the Ga atoms at 450 °C, until a proper $\sqrt{3}\times\sqrt{3}$ surface reconstruction was seen on RHEED.

The films were subsequently grown at a substrate temperature of about 450 °C and with a Se/Ga flux ratio between 8 and 9. The growth speed was about 11 Å/mn. Shortly after the beginning of the growth (2 to 3 sec), the original RHEED reconstruction (1×1 H-Si, 7×7-Si or $\sqrt{3}\times\sqrt{3}$ Ga-Si) faded away and was replaced by a 1×1 reconstruction whose parameter matches the Si parameter (1×1-Si). This reconstruction remains until about 40 sec growth (one GaSe layer coverage) where the RHEED diffraction lines gradually move to a 1×1 reconstruction with a lateral parameter close to the bulk GaSe lateral parameter (1×1-GaSe).

Six samples were studied for the present work. Four of them grown on H-Si(111) will be referred to as H_0, H_1, H_2 and H_3-Si; the two others deposited on $\sqrt{3}\times\sqrt{3}$ Ga-Si(111) and 7×7-Si(111) will be noted Ga-Si and 7×7-Si.

As already reported,[19] air exposition induces a slow degradation of the films. To minimize this effect, the samples

TABLE I. GaSe coverage. θ_f, Ga coverage deduced from fluorescence data and coherent fraction measurements; θ_r, Ga coverage extracted from RBS experiments.

Sample	I_{Ga} (a.u.)	I_{Se}/I_{Ga}	% Ga	θ_f (ML)	% Ga RBS	θ_r (ML) RBS
Ga-Si	2140 ± 180	1.97 ± 0.15	52 ± 7	0.9 ± 0.1	49 ± 9	0.9 ± 0.1
7×7-Si	2815 ± 220	1.66 ± 0.20	48 ± 8	1.2 ± 0.1		
H_1-Si	4360 ± 270	1.91 ± 0.15	51 ± 8	1.9 ± 0.1	52 ± 3	1.7 ± 0.1
H_2-Si	6920 ± 330	1.71 ± 0.15	48 ± 8	2.9 ± 0.1		
H_3-Si	7400 ± 400	1.98 ± 0.15	52 ± 7	3.1 ± 0.2	51 ± 3	3.4 ± 0.2

were manipulated in a N_2-filled chamber and a x-ray experimental cell, swept by a N_2 flux, was used during x-ray exposition. Under those conditions, film degradation occurs in several days instead of a few hours when exposed in ambient atmosphere. We would like to point out the quite low reactivity of the samples, as their 1×1 reconstructions seen by RHEED immediately appear upon reentry in the UHV chamber after being exposed for several hours to ambient atmosphere. Those properties were observed by other authors.[20]

C. Experimental setup

The experiments were conducted on beamline D25B of the storage ring DCI in LURE (Orsay, France) using incident beams ranging from 0.9 to 1.15 Å, in order to obtain an incident radiation near Ga (1.19 Å) or Se (0.98 Å) absorption edge. To obtain a beam of tunable wavelength, with little energy dispersion, monolithic grooved four-reflection monochromators were used.[21] The nondispersive setting requires that each substrate reflection is recorded using a specially designed monochromator using the same material and reflection of the sample's substrate. The XSW analysis can thus only be performed for a small number of reflections (in our case, 111, 220, and 113 reflections). That is why we obtained less information about the Se position than for the Ga using 111 reflection, because the wavelength is too short and the Bragg angles too small to construct a monochromator that fits into the monochromator chamber. Experimental and theoretical details about the XSW technique may be found elsewhere.[22]

III. RESULTS AND DISCUSSION

A. GaSe coverage

After XSW experiments, the x-ray fluorescence spectrum was recorded for five samples, apart from the reflectivity curve, in order to obtain an x-ray fluorescence dosage. The results are shown in Table I. The given Ga percentages were calculated, assuming an infinitely thin atomic distribution, the Se-Ga fluorescence counts ratio I_{Se}/I_{Ga} being, for the 50%/50% composition,

$$\frac{I_{Se}}{I_{Ga}}=\frac{\mu_{Se}(\lambda)P_{K_\alpha}(Se)}{\mu_{Ga}(\lambda)P_{K_\alpha}(Ga)}=\frac{19310\times0.597}{12370\times0.508}=1.83. \quad (4)$$

The K-shell fluorescence probabilities P_{K_α} ratios were calculated using the approximation given in Ref. 22. The overall absorption coefficients μ were estimated using the Cromer[23] program.

The Ga coverage θ_f is proportional to I_{Ga}. The proportionality constant is evaluated using coherent fraction measurements as seen in the next section. θ_f ranges from 0.9 for the thinner sample to 3.1 for the thicker.

These values were cross checked for three samples with Rutherford back-scattering (RBS) elements dosage. As the atomic number of Ga and Se are very close, the two RBS element peaks are difficult to separate, even using 2.2 MeV He_4^2 ions. However, the results are in good agreement for both methods. The absolute reference of RBS dosage confirms the value of 0.9 Ga monolayer for the Ga-Si sample. Therefore, this sample will be used as a standard for the interface structure determination.

B. Ga fluorescence

1. Interface structure

A first series of XSW measurements was performed on the thinner samples in order to determine the interface structure.

The results are displayed in Table II. It shows the coefficients F and P for the investigated reflections (parallel 111 and inclined 220 and 113). The number n gives the order in which each experiment was performed; we will take this into account to explain the loss of coherence due to non-UHV environment. The given errors vere calculated using the dispersion of measured fluorescence counts among each acquisition. This error type arises from systematic shifts in the piezoelectric rocking system. For these experiments, the fluorescence counts were high enough to discard the standard

TABLE II. Coherent fractions and positions for the thinner films. Estimated errors are ±0.01 for P and ±0.02 for F. The integer n gives the order in which the experiments were conducted.

Surface	n	Reflection	P_{Ga}	F_{Ga}	P_{Se}	F_{Se}
H_0-Si	1	111	0.88	0.63		
	2	220	0.03	0.70		
	3	111[a]	0.89	0.40	0.21	0.44
7×7-Si	1	111	0.87	0.76		
	3	220	0.02	0.38	0.07	0.32
	2	113	0.12	0.67	0.08	0.44
Ga-Si	1	111	0.89	0.95		
	2	220	0.03	0.87	0.12	0.68
	3	113	0.15	0.38	0.10	0.34

[a]Experiments performed using a less reliable two-reflection monochromator at wavelength $\lambda=0.89$ Å.

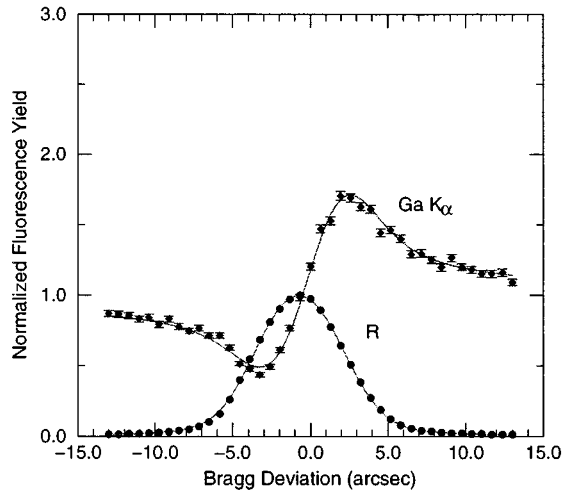

FIG. 2. Ga-Si sample. Experimental data and fitted curves for the Ga K_α normalized fluorescence yield and x-ray reflectivity R. 111 reflection parallel to the interface, $\lambda = 1.13$ Å. Deduced values are $F_{111}^{\mathrm{Ga}} = 0.95 \pm 0.02$ and $P_{111}^{\mathrm{Ga}} = 0.89 \pm 0.01$

statistical error, only leaving the dispersion error. The given relative errors of 2% for F values and 1% for P values are the biggest errors calculated for all the presented experiments.

a. Results for the Ga-Si sample. The XSW spectra of this sample are displayed in Fig. 2 for the 111 reflection parallel to the interface and on Fig. 3 for an inclined 220 reflection. For 111 reflection, the coherent fraction is near the theoretical maximum when thermal displacements of the Si surface atoms are taken into account. This implies that: (1) the Ga site has a unique position, (2) the distribution of the Ga atoms around the mean position is sharp edged, and (3) the sample was not significantly degraded during the experiment.

Using both parallel and inclined reflections, the Ga atoms were located at 2.37 ± 0.03 Å above the top silicon atoms of

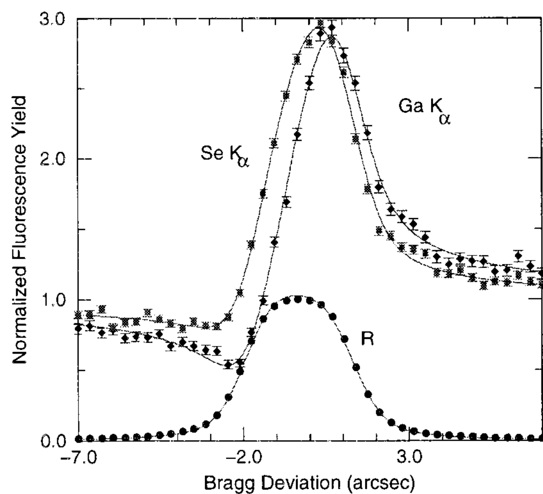

FIG. 3. Ga-Si sample. Experimental data and fitted curves for the Ga and Se K_α normalized fluorescence yields and x-ray reflectivity R. 220 reflection, $\lambda = 0.95$ Å. Deduced values are $F_{220}^{\mathrm{Ga}} = 0.87 \pm 0.02$ and $P_{220}^{\mathrm{Ga}} = 0.03 \pm 0.01$, $F_{220}^{\mathrm{Se}} = 0.68 \pm 0.02$, and $P_{220}^{\mathrm{Se}} = 0.12 \pm 0.01$

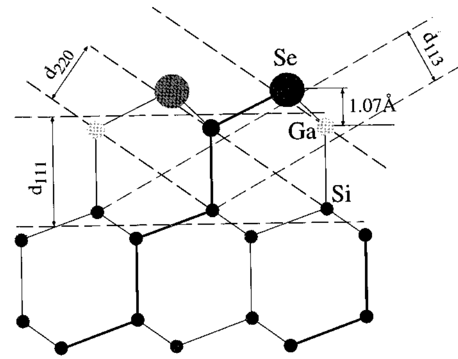

FIG. 4. Schematic drawing of the interface structure. The GaSe half-layer is constrained on the Si substrate. Se atoms lie at the Si surface S site.

the unrelaxed Si(111) surface. This value is consistent with a Si-Ga bond between a top Si atom and a Ga in the T site (Fig. 4).

It should be pointed out that, even under N_2 flux, a loss of coherence of the film is detected between the first ($n = 1$) and the last ($n = 3$) XSW experiment. However, taking into

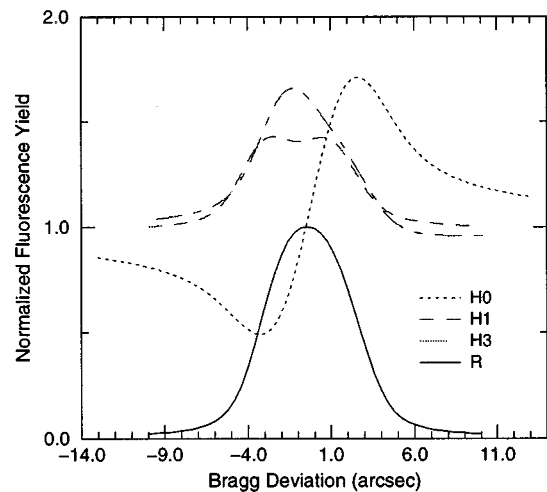

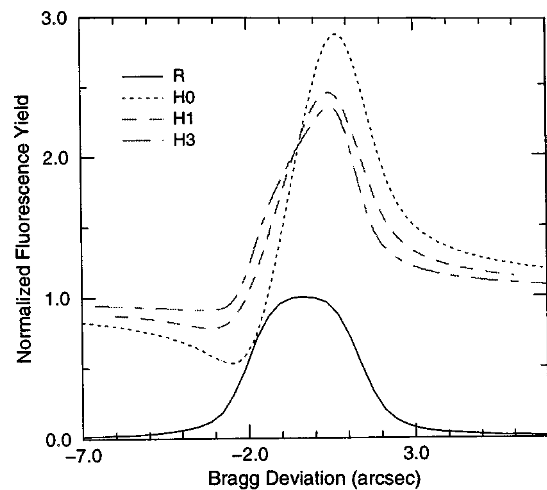

FIG. 5. Experimental data for the Ga and Se K_α normalized fluorescence yields for H_0, H_1, and H_3-Si samples. (a) 111 reflection, $\lambda = 1.13$ Å; a drastic evolution of the curve is observed. (b) 220 reflection, $\lambda = 0.95$ Å; the curves shapes are very similar.

TABLE III. Coherent fractions and positions for higher GaSe coverages. Estimated errors are ±0.01 for P and ±0.02 for F. θ represents the Ga coverage.

Sample	n	Refl	P_{Ga}	F_{Ga}	P_{Se}	F_{Se}	θ (ML)
H_1-Si	1	111	0.76	0.29			1.9
	2	220	0.02	0.54	0.09	0.41	
	3	113	0.14	0.45	0.11	0.32	
H_2-Si	3	111	0.63	0.30			2.9
	1	220	0.02	0.35	0.07	0.31	
	2	113	0.14	0.29	0.12	0.23	
H_3-Si	1	111	0.65	0.25			3.1
	2	220	0.03	0.32	0.06	0.24	
	3	113	0.15	0.23	0.15	0.14	

account all experimental data, it appears that the degradation affects mainly the coherent fraction and less the coherent position.

b. Results for the other thinner samples. Ga-Si, 7×7-Si and H_0-Si samples have similar values for $P_{\vec{h}}^{Ga}$ coefficients in all investigated reflections. This implies the same interface structure, whatever the Si surface preparation. This is an important conclusion. It appears clearly that the epitaxy between GaSe and Si(111) is not a ''van der Waals epitaxy'' but a ''classical'' pseudomorphic epitaxy. The results of the Ga-Si sample show a clear modification of the Ga atoms positions from the $\sqrt{3}\times\sqrt{3}$ Ga-Si(111) for the clean Si surface to the measured position.

2. Growth beyond the interface

The second experimental series of XSW experiments dealt with GaSe films of increasing coverages. The results are summarized in Table III. As shown in Fig. 5, using the 111 parallel reflection the fluorescence yield changes with increasing coverage, whereas using the inclined 220 reflection it almost does not vary. Consequently with the parallel reflection, the XSW detect all Ga planes, while with inclined reflection, only the interface plane is seen. This can be achieved if, beyond the interface, the GaSe in-plane parameter is not commensurate with the Si surface parameter. In fact, this result strengthens the hypothesis of a GaSe half-layer grafted on the Si surface. Indeed, if this half-layer is strained, the upper layer should be relaxed due to the weak van der Waals interactions between those two entities.

This is confirmed by the $F_{\vec{h}}^{Ga}$ values analysis. Assuming such a relaxation, the $F_{\vec{h}}^{Ga}$ values, if they are equal for 220 and 113 inclined reflections, are a direct measure of the Ga coverage. This is possible in this case, because the lateral positions for the upper layer can have any value and only the half-layer atoms contributes to the $F_{\vec{h}}$ and $P_{\vec{h}}$ values. In this case, the coherent fraction is simply

$$F_{hkl\neq 111}=\frac{f_0}{\mathcal{N}}\equiv\frac{f_0}{\theta}, \tag{5}$$

where f_0 is the coherent fraction of the half-layer alone and the number $\mathcal{N}$ is the number of adsorbate atoms above the surface divided by the number of coherent atoms (i.e., the Ga coverage expressed in monolayers).

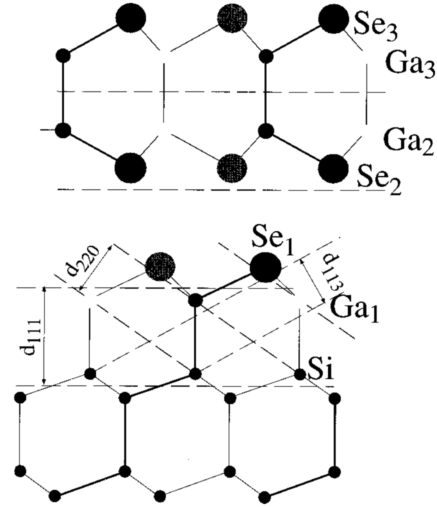

FIG. 6. Schematic drawing of a thin heteroepitaxy (θ = 3.0 ML). Ga_1, Se_1, Ga_2, and Ga_3 are the atoms starting from the nearest to Si, their vertical positions are described in the text.

Using this relation, and taking only into account the first experiment ($n=1$) to limit the effect of the non-UHV environment, we obtain a minimal value for the Ga coverage θ. The values calculated for the different samples are shown in Table III. They agree rather well with those deduced from fluorescence and RBS experiments shown in Table I. Therefore, the assumption of noncommensurability is confirmed.

Moreover, another feature of the GaSe growth can be extracted from the XSW data. By using a value of 7.94 Å for the thickness of a GaSe layer (defined in Fig. 1) and the vertical position of Se_1 (see Fig. 6) measured in Sec. III C, the vertical positions of Ga_2 and Ga_3 (also in Fig. 6) are 5.45 and 7.84 Å. If those values are used to simulate the coherent position and coherent fraction of the Ga atoms for a film consisting of one half-layer plus an entire layer, it comes to

$$F_{111}e^{2i\pi P_{111}}=\tfrac{1}{3}\,e^{2i\pi 0.89}\left[1+e^{2i\pi(7.84\sqrt{3}/5.431)}+e^{2i\pi(5.45\sqrt{3}/5.431)}\right]. \tag{6}$$

This formula gives $P_{111}^{Ga}=0.65$ and $F_{111}^{Ga}=0.32$, two values very close to those found for the H_3-Si ($\theta=3.0$ ML) sample (Table IV). If a variable coverage is considered, the calculated values for $\theta=1.8$ ML are $P_{111}^{Ga}=0.76$ and $F_{111}^{Ga}=0.34$; values very close to the experimental ones. Finally, it appears a good agreement between simulations and observations, especially for coherent positions.

This agreement gives the key to elucidate the growth mode after the deposition of the interface half-layer. An entire layer in the sequence Se-Ga-Ga-Se is growing until the surface is covered. The growth does not proceed atomic plane by atomic plane.

C. Se fluorescence

The key problem with the Se fluorescence is the determination of the Se position. As seen in the structural section, there are two possible options to place the Se atoms: Si-like or GaSe-like.

A first analysis of the collected data reported in Tables II and III locates a Se atom on a vertical line running through

TABLE IV. Comparison between experimental and calculated results. θ: Ga coverage deduced from relation (5).

Sample	n	Reflection	P_{Ga} Experiment	F_{Ga} Experiment	P_{Ga} Model	F_{Ga} Model	θ
Ga-Si	1	111	0.89	0.95	0.89	0.99	<1
	2	220	0.03	0.87	0.06	0.97	
	3	113	0.15	0.38	0.15	0.96	
7×7-Si	1	111	0.87	0.76	0.87	0.75	1.1
	3	220	0.02	0.38	0.06	0.84	
	2	113	0.12	0.67	0.15	0.83	
H_1-Si	1	111	0.76	0.29	0.76	0.34	1.8
	2	220	0.02	0.54	0.06	0.54	
	3	113	0.14	0.45	0.15	0.53	
H_2-Si	3	111	0.63	0.30	0.63	0.34	2.8
	1	220	0.02	0.35	0.06	0.34	
	2	113	0.14	0.29	0.15	0.34	
H_3-Si	1	111	0.65	0.25	0.65	0.32	3.0
	2	220	0.03	0.32	0.06	0.32	
	3	113	0.15	0.23	0.15	0.32	

the center of the triangle formed by three Ga interface atoms whatever the Si surface preparation.

The vertical position of the Se atom is found to be 1.07 Å above the Ga interface atoms, distance shorter than in bulk GaSe. This is not surprising, since the Ga triangle has been expanded by 2.6%, to match the Si surface parameter. If the Ga-Se bonding lengths are kept constant, the Ga lateral expansion lead to a Se theoretical position 1.08 Å above the Ga interface atom. The found position of 1.07 Å is in good agreement with this model.

The lateral Se position matches at the interface with the site S of the silicium surface. With this assumption, the half-layers should be in the Si-like configuration illustrated in Fig. 1. However, the Se distribution at the interface seems more complicated: (1) Se lateral positions deduced from 220 and 113 reflections do not cross check very well, whereas there is a good agreement between those reflections for the Ga interface atoms; (2) There is a large dispersion of the measured positions, while there is almost no dispersion for the Ga measurements.

One way to solve this dilemma is to introduce at the interface a proportion of Se atoms in the GaSe-like configuration. To do that will hopefully induce in some areas the stacking of layers in the GaSe-like configuration. The calculated positions as a function of the Si-like configuration percentage are shown in Table V. The experimental values for each sample can be explained in assuming a different percentage. Proportions are found to be 85/15 for the Ga-Si sample, 75/25 for H_1-Si and H_2-Si, 70/30 for H_3-Si.

TABLE V. F_{Se} and P_{Se} values for 220 and 113 reflections assuming variable proportions of Si and GaSe-like configurations.

% Si-like	P_{220}^{Se}	F_{220}^{Se}	P_{113}^{Se}	F_{113}^{Se}
85	0.12	0.79	0.08	0.79
80	0.11	0.72	0.10	0.72
75	0.09	0.66	0.11	0.66
70	0.07	0.61	0.13	0.61

However, this proportion of another site occupancy at the interface cannot explain the bigger proportion of almost 50/50 for the two stacking orientations found by HRTEM or by grazing incidence x-ray diffraction on thicker (5 and 7 ML) samples.[24] This implies that the stacking sequences may start at the interface, perhaps with Si-like and GaSe-like half-layer configurations but also further due to the occurence of stacking faults.

IV. CONCLUSIONS

In conclusion, the XSW technique has shown the interface structure of the GaSe/Si(111) heteroepitaxy to consist of a GaSe half-layer grafted onto the Si(111) surface. Whatever the initial surface preparation, i.e., H-Si(111), 7×7-Si(111), or $\sqrt{3}\times\sqrt{3}$ Ga-Si(111), the interface structure is the same. Ga atoms are covalently bonded with Si top atoms while upper Se atoms occupy two different sites. Beyond the interface, the growth proceeds layer by layer and not atomic plane by atomic plane. Finally, after the interface, the first entire Se-Ga-Ga-Se layer is almost relaxed with respect to the Si substrate and the distance between the half-layer and the first complete layer is consistent with the bulk γ-GaSe structure.

ACKNOWLEDGMENTS

We would like to thank C. Cohen and F. Abel from the GPS (Universities Paris 7 and Paris 6, Jussieu, France) for their kind help during the RBS measurements.

*Also at L.U.R.E., CNRS-MEN-CEA, Bat. 209D, 91405 Orsay, France.

[1] N. Fernelius, *Progress in Crystal Growth and Characterisation* (Elsevier, North-Holland, 1994), Vol. 28, p. 275.
[2] N. Singh *et al.*, J. Cryst. Growth **163**, 398 (1996).
[3] A. Koma, K. Sunouchi, and T. Miyajima, J. Vac. Sci. Technol. B **3**, 724 (1985).
[4] O. Lang *et al.*, J. Appl. Phys. **75**, 7805 (1994).
[5] O. Lang *et al.*, J. Appl. Phys. **75**, 7814 (1994).
[6] K. Ueno, H. Abe, K. Saiki, and A. Koma, Jpn. J. Appl. Phys. **30**, 1352 (1991).
[7] F. Ohuchi *et al.*, J. Cryst. Growth **111**, 1033 (1991).
[8] J. Palmer, T. Saitoh, T. Yodo, and M. Tamura, J. Appl. Phys. **74**, 7211 (1993).
[9] K. Liu *et al.*, Jpn. J. Appl. Phys. **32**, 434 (1993).
[10] L. T. Vinh *et al.*, J. Cryst. Growth **135**, 1 (1994).
[11] J. Palmer, T. Saitoh, T. Yodo, and M. Tamura, J. Cryst. Growth **147**, 283 (1995).
[12] A. Koëbel *et al.*, J. Cryst. Growth **154**, 269 (1995).
[13] B. Batterman, Phys. Rev. **A759**, 133 (1964).
[14] B. Batterman, Phys. Rev. Lett. **22**, 703 (1969).
[15] S. Andersen, J. Golovchenko, and G. Mair, Phys. Rev. Lett. **37**, 1141 (1976).
[16] P. Cowan, J. Golovchenko, and M. Robbins, Phys. Rev. Lett. **44**, 1680 (1980).
[17] K. Schubert, E. Dorre, and M. Kluge, Zur Kristalch. der B-Met. III **46**, 216 (1970).

[18] A. Kuhn, A. Chevy, and R. Chevalier, Phys. Status Solidi A **31**, 469 (1975).
[19] Y. Zheng *et al.*, J. Cryst. Growth **162**, 135 (1996).
[20] K. Ueno, N. Takeda, K. Sasaki, and A. Koma, Appl. Surf. Sci. **113/114**, 38 (1997).
[21] J. Boulliard *et al.*, J. Phys. I **2**, 1205 (1992).
[22] J. Zegenhagen, Surf. Sci. Rep. **18**, 199 (1993).
[23] D. Cromer, J. Appl. Crystallogr. **16**, 437 (1983).
[24] N. Jedrecy, R. Pinchaux, and M. Eddrief, Phys. Rev. B (to be published).